Regional fibre stress : fibre strain area as an estimate of regional blood flow and oxygen demand in the canine heart

Regional fibre stress–fibre strain area as an estimate of regional blood flow and oxygen demand in the canine heart

Tammo Delhaas, Theo Arts*, Frits W. Prinzen and Robert S. Reneman

*Departments of Physiology and *Biophysics, Cardiovascular Research Institute Maastricht, University of Limburg, PO Box 616, 6200 MD Maastricht, The Netherlands*

1. In the present study the relation between regional left ventricular contractile work, regional myocardial blood flow and oxygen uptake was assessed during asynchronous electrical activation.

2. In analogy to the use of the pressure–volume area for the estimation of global oxygen demand, the fibre stress–fibre strain area, as assessed regionally, was used to estimate regional oxygen demand. The more often used relation between the pressure–sarcomere length area and regional oxygen demand was also assessed.

3. Experiments were performed in six anaesthetized dogs with open chests. Regional differences in mechanical work were generated by asynchronous electrical activation of the myocardial wall. The ventricles were paced from the right atrium, the left ventricular free wall, the left ventricular apex or the right ventricular outflow tract. Regional fibre strain was measured at the epicardial anterior left ventricular free wall with a two-dimensional video technique.

4. Regional fibre stress was estimated from left ventricular pressure, the ratio of left ventricular cavity volume to wall volume, and regional deformation. Total mechanical power (TMP) was calculated from the fibre stress–fibre strain area (SSA) and the duration of the cardiac cycle (t_{cycle}) using the equation: $TMP = SSA / t_{cycle}$. Regional myocardial blood flow was measured with radioactive microspheres. Regional oxygen uptake was estimated from regional myocardial blood flow values and arteriovenous differences in oxygen content.

5. During asynchronous electrical activation, total mechanical power, pressure–sarcomere length area, myocardial blood flow and oxygen uptake were significantly lower in early than in late activated regions ($P < 0{\cdot}05$).

6. Within the experiments, the correlation between the pressure–sarcomere length area and regional oxygen uptake was not significantly lower than the one between total mechanical power (TMP) and regional oxygen uptake ($\dot{V}_{O_2,reg}$). However, variability of this relation between the experiments was less for total mechanical power. Pooling all experimental data revealed: $\dot{V}_{O_2,reg} = k_1 TMP + k_2$, with $k_1 = 4{\cdot}94 \pm 0{\cdot}31$ mol J^{-1} and $k_2 = 24{\cdot}2 \pm 1{\cdot}9$ mmol m^{-3} s^{-1} (means ± standard error of the estimate).

7. This relation is in quantitative agreement with previously reported relations between the pressure–volume area and global oxygen demand. The results indicate that asynchronous electrical activation causes a redistribution of mechanical work and oxygen demand and that regional total mechanical power is a better and more general estimate of regional oxygen demand than the regional pressure–sarcomere length area.

The relationship between global mechanical work and oxygen demand has been widely investigated in the left ventricle (Braunwald, 1971; Parmley & Tyberg, 1976; Weber, 1979; Panerai, 1980). Suga and co-workers proposed a method to estimate global oxygen demand from the pressure–volume area of the left ventricle (Suga, 1979; Suga, Hayashi & Shirahata, 1981*a*; Suga, Hayashi, Shirahata, Suehiro & Hisano, 1981*b*). The pressure–volume area is defined as the area bounded by the pressure–volume trajectory during systole and both the end-systolic and end-diastolic pressure–volume relationship curves. For a wide range of conditions, the pressure–volume area is closely related to myocardial oxygen consumption (Khalafbeigui, Suga & Sagawa, 1979; Suga *et al.* 1981*b*;

Suga, Hisano, Hirata, Hayashi, Yamada & Ninomiya, 1983; Hata, Goto & Suga, 1991).

Several methods to estimate regional contractile work in the left ventricle in the control situation as well as during ischaemia or asynchronous electrical activation have been proposed (Theroux, Franklin, Ross & Kemper, 1974; Tyberg, Forrester, Wyatt, Goldner, Parmley & Swan, 1974; Badke, Boinay & Covell, 1980; Gallagher, Osakada, Matsuzaki, Kemper & Ross, 1982; Lew, 1987). In one method, left ventricular pressure is plotted as a function of regionally measured segment length (Theroux *et al.* 1974; Tyberg *et al.* 1974). Another method (Gallagher *et al.* 1982; Lew, 1987) uses values of calculated regional stress and unidirectionally measured segmental shortening. In both methods, generation of mechanical work is indicated by the presence of a loop. However, in none of the studies mentioned was an attempt made to relate the indices of regional work to regional oxygen demand.

In analogy to the pressure–volume area concept for the global left ventricle, regional oxygen demand may be determined from the regional fibre stress–fibre strain area. The pressure–volume area and the regional fibre stress–fibre strain areas are related as follows: the sum of the regional fibre stress–fibre strain areas for the individual muscle fibres that constitute a ventricle is equal to the pressure–volume area of that ventricle. In experiments on isolated ferret papillary muscle, the force–length area (the analog of the pressure–volume area for a linear muscle) was found to be closely related to oxygen consumption (Hisano & Cooper, 1987). These findings suggest that the regional fibre stress–fibre strain area can be used to estimate regional oxygen demand.

In the present study it was investigated, in anaesthetized dogs with open chests, whether the left ventricular pressure–sarcomere length area or the fibre stress–fibre strain area is the best predictor of regional oxygen demand. To address this question, the determination of global haemodynamics, and regional fibre stress and fibre strain is required. Regional fibre strain can be measured accurately in the subepicardial layers by determining planar deformation at the epicardial surface (Arts & Reneman, 1980; Prinzen, Arts, Prinzen & Reneman, 1986*b*). Direct measurement of regional fibre stress is practically impossible, because the insertion of transducers into the wall damages the tissue at the site of measurement (Feigl, Simon & Fry, 1967; Huisman, Elzinga, Westerhof & Sipkema, 1980). Therefore, a modification of an earlier model of cardiac mechanics (Arts, Veenstra & Reneman, 1982; Arts, Bovendeerd, Prinzen & Reneman, 1991) was used to estimate regional fibre stress during systole from experimentally measured left ventricular pressure, left ventricular cavity volume, and regionally measured fibre strain. Subepicardial fibre strain was assessed at the epicardial surface of the anterior left ventricular free wall, using a two-dimensional video technique (Prinzen *et al.* 1986*b*). Ventricular pacing from various sites was used as an intervention to obtain regional differences in mechanical performance (Wiggers, 1925; Lister, Klotz, Jomain, Stuckey & Hoffman, 1964; Badke *et al.* 1980; Prinzen, Augustijn, Arts, Allessie & Reneman, 1990; Delhaas, Arts, Prinzen & Reneman, 1993*b*). Regional oxygen uptake was estimated from regional myocardial blood flow as determined by radioactively labelled microspheres, and measured arterio-coronary sinus differences in oxygen content.

METHODS

Estimation of regional fibre stress

In the present study a modification of the model of Arts and co-workers (Arts *et al.* 1982, 1991) was used to estimate regional fibre stress. In the original model it was found that during ejection the dimensionless ratio of left ventricular pressure (P_{lv}) and mean Cauchy fibre stress (σ_f), averaged over the left ventricular wall, which is force per actual cross-sectional area of the muscle fibre bundle, can be approximated by the dimensionless ratio of left ventricular cavity (V_{lv}) to wall volume (V_w):

$$\frac{\sigma_f}{P_{lv}} = 1 + 3\frac{V_{lv}}{V_w}. \quad (1)$$

Furthermore, during ejection mean sarcomere length ($\bar{L}_s$), averaged over the left ventricular wall, depends solely on the instantaneous ratio of left ventricular cavity volume to left ventricular wall volume (Arts *et al.* 1982, 1991):

$$\frac{\bar{L}_s}{L_{s,V_{lv}=0}} = \left(1 + 3\frac{V_{lv}}{V_w}\right)^{1/3}, \quad (2)$$

where $L_{s,V_{lv}=0}$ represents sarcomere length at extrapolated zero left ventricular cavity volume. In the present study, the length of the cardiac muscle fibre was quantified in terms of estimated sarcomere length.

During asynchronous electrical activation, large differences in regional fibre shortening and, hence, in regional cross-sectional area are found (Badke *et al.* 1980; Prinzen *et al.* 1990; Delhaas *et al.* 1993*b*). This results in regional differences in Cauchy fibre stress. To estimate regional Cauchy fibre stress in a non-uniformly contracting ventricle, the following additional assumptions were made. (1) In the reference situation, myocardial fibres do not cross and follow pathways with zero divergence (Chadwick, 1982). Then Cauchy fibre stress is homogeneous. (2) During contraction, force along a given myocardial bundle is the same everywhere, due to a free conductance of force along the fibres. Thus the force per original cross-sectional area, the so called first Piola–Kirchhoff stress, τ_f, is homogeneously distributed throughout the ventricular wall.

Due to tissue incompressibility, average sarcomere length is inversely proportional to the cross-sectional area of the fibre. Thus for τ_f it holds:

$$\tau_f = \sigma_f \frac{L_{s,V_{lv}=0}}{\bar{L}_s}. \quad (3)$$

Applying eqns (1) and (2) to eqn (3), for τ_f in the left ventricle it is found:

$$\tau_f = P_{lv}\left(1 + 3\frac{V_{lv}}{V_w}\right)^{2/3}. \quad (4)$$

Correcting eqn (4) with fibre strain as regionally measured with respect to the configuration at extrapolated zero cavity

volume ($L_{s,reg}/L_{s,V_{lv}=0}$), regional Cauchy fibre stress ($\sigma_{f,reg}$) may be expressed in experimentally measurable quantities:

$$\sigma_{f,reg} = P_{lv}\left(1 + 3\frac{V_{lv}}{V_w}\right)^{2/3} \frac{L_{s,reg}}{L_{s,V_{lv}=0}}. \quad (5)$$

Estimation of regional sarcomere length

Calculation of fibre stress from fibre strain by use of the constitutive relation of myocardial tissue requires estimation of regional sarcomere length. The following assumptions were used. (1) Sarcomere length at zero left ventricular transmural pressure in the passive state ($L_{s,eq}$) equals 1·95 μm (Spotnitz, Sonnenblick & Spiro, 1966; Grimm, Lin & Grimm, 1980), while the corresponding left ventricular cavity volume is defined as $V_{lv,eq}$. (2) In the systolic phase, if left ventricular cavity volume equals $V_{lv,eq}$, sarcomere length remains as $L_{s,eq}$. (3) In the synchronously activated left ventricle, fibre shortening and, hence, sarcomere shortening is homogeneous during the

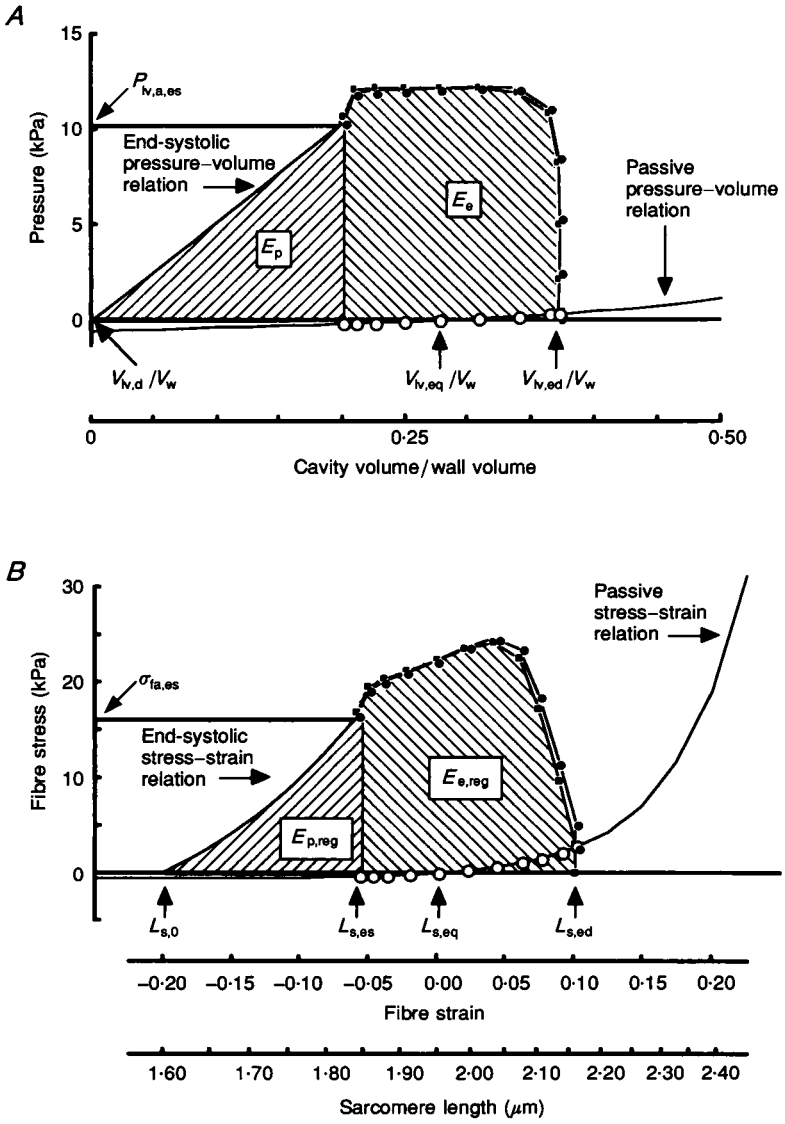

Figure 1. Analogy between pressure–volume area and fibre stress–fibre strain area

Myocardial oxygen demand may be determined globally (*A*) as well as regionally (*B*) from the mechanical work performed. In *A*, left ventricular pressure is plotted as a function of left ventricular cavity volume normalized to wall volume. Myocardial oxygen demand correlates with the pressure–volume area (PVA). This PVA is the sum of the external mechanical work E_e and the so-called potential mechanical work E_p, which is related to end-systolic pressure (Suga, 1979; Suga *et al.* 1981*a*, *b*). Abbreviations: $P_{lv,a,es}$ is end-systolic active left ventricular pressure; $V_{lv,d}$ and $V_{lv,eq}$ are left ventricular cavity volume at zero end-systolic left ventricular pressure and at passive zero transmural pressure, respectively; V_w is wall volume. Cavity volume is normalized to wall volume. ●, P_{lv}; ■, $P_{lv,a}$. In *B*, fibre stress is plotted as a function of fibre strain. On the horizontal axis, calculated sarcomere length is also indicated. Regional myocardial oxygen uptake has been correlated with the regional SSA, being the sum of the regional external mechanical work ($E_{e,reg}$) and the regional potential mechanical work ($E_{p,reg}$). Abbreviations: $\sigma_{fa,es}$ is end-systolic active fibre stress; $L_{s,0}$, $L_{s,es}$, $L_{s,eq}$, and $L_{s,ed}$ represent sarcomere length at zero active fibre stress, at end-systole, at passive zero transmural pressure and at end-diastole, respectively. ●, σ_f; ■, σ_{fa}.

ejection phase (Delhaas, Arts, Bovendeerd, Prinzen & Reneman, 1993*a*). Therefore, sarcomere length at mid-ejection of the control beat ($L_{s,ref}$), which is the reference state for the deformation measurements, can be calculated by:

$$L_{s,ref} = L_{s,eq}\left(\frac{1+3(V_{lv,ref}/V_w)}{1+3(V_{lv,eq}/V_w)}\right)^{1/3}. \quad (6)$$

Regional sarcomere length is calculated from regionally measured strain differences between the control and the actual state.

Estimation of regional contractile work and energy demand

The first index of regional contractile work used in this study was the pressure–sarcomere length area, which is the area bounded by the systolic limb of the pressure–sarcomere length loop trajectory and the x-axis (Theroux *et al.* 1974; Tyberg *et al.* 1974).

The second index used was the fibre stress–fibre strain area, a regional analogue of the model presented by Suga and co-workers (Suga, 1979; Suga *et al.* 1981*a*, *b*). In this model, the total amount of mechanical energy needed for the left ventricle to contract from end-diastolic to end-systolic volume is the sum of the external mechanical work (E_e) and the so-called end-systolic potential work (E_p). This combined area is equal to the pressure–volume area, which is the area bounded by the end-systolic and end-diastolic pressure–volume curves and the systolic limb of the pressure–volume loop trajectory (Fig. 1*A*). The intersection of the end-systolic pressure–volume curve and the x-axis is denoted by $V_{lv,d}$. Below this volume no active pressure can be developed. The relation between the pressure–volume area (PVA) and the global oxygen demand ($\dot{V}_{O_2}$) was described by a linear equation:

$$\dot{V}_{O_2} = c_1 \mathrm{PVA} + c_2, \quad (7)$$

where c_1 represents a conversion constant of mechanical work to oxygen demand and c_2 the oxygen required by the left ventricle for basal metabolism plus excitation–contraction coupling.

Analogously, regional oxygen demand in the left ventricular tissue is assumed to be proportional to the regional fibre stress–fibre strain area (Fig. 1*B*). The regional fibre stress–fibre strain area was calculated as follows. (1) Using eqn (5), regional Cauchy fibre stress was calculated from left ventricular pressure, the ratio of left ventricular cavity volume to wall volume, and sarcomere length estimated according to the above-mentioned method. (2) Neglecting the viscous behaviour of passive myocardial fibres, the relation between passive fibre stress (σ_{fp}) and sarcomere length (L_s) is described by:

$$\sigma_{fp} = \sigma_{fp0}(\exp\{b(L_s - L_{s,eq})\} - 1), \quad (8)$$

in which $L_{s,eq}$, b and σ_{fp0} are parameters. The parameter b governs the exponential increase of σ_{fp} with increasing sarcomere length. Based on experiments on isolated cat papillary muscle, the value of b was assumed to be 8 μm^{-1} (ter Keurs, Rijnsburger, van Heuningen & Nagelsmit, 1980; van Heuningen, Rijnsburger & ter Keurs, 1982). For each separate experiment, the value of σ_{fp0} was calculated from end-diastolic left ventricular pressure and left ventricular cavity volume as measured in the control situation, applying eqns (1) and (2). (3) The active component of regional fibre stress during systole (σ_{fa}) was obtained by subtracting passive fibre stress (eqn (8)) from total fibre stress (eqn (5)). (4) Regional external work during systole ($E_{e,reg}$) was calculated from the area bounded by the systolic limb of the active fibre stress–fibre strain loop trajectory and the x-axis (Fig. 1*B*). (5) The regional potential work term $E_{p,reg}$ (Suga, 1979; Suga *et al.* 1981*a*, *b*) was estimated from the area bounded by the end-systolic fibre stress–fibre strain relation and the x-axis. (6) Finally, the regional fibre stress–fibre strain area SSA was calculated as:

$$\mathrm{SSA} = E_{e,reg} + E_{p,reg}. \quad (9)$$

Regional total mechanical power (TMP) was calculated from

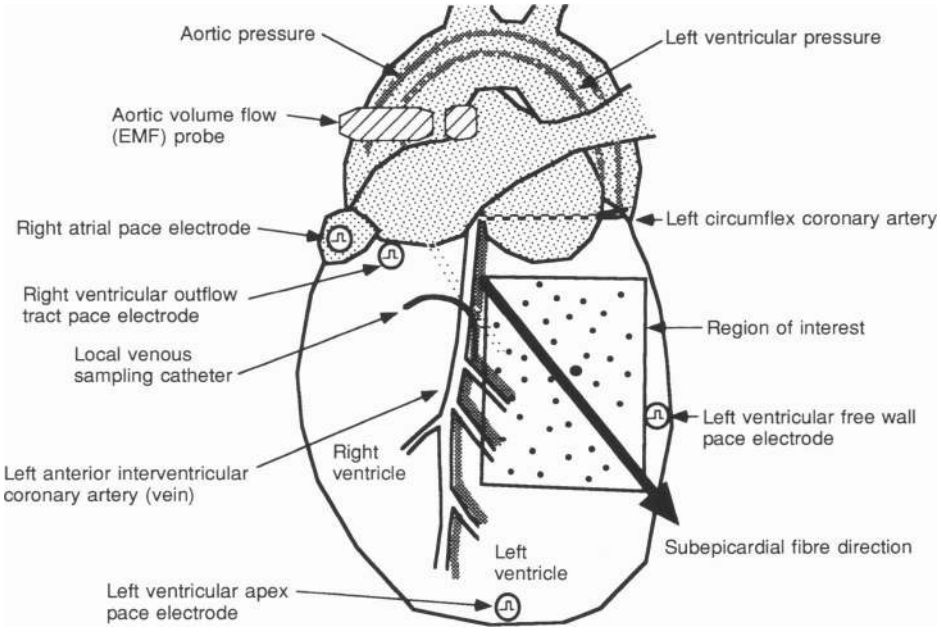

Figure 2. Schematic representation of experimental set-up

The dots within the area of interest are optical markers, attached to the epicardial surface. The sampling catheter in the coronary sinus is not depicted.

the regional fibre stress–fibre strain area (SSA) and the duration of the cardiac cycle (t_{cycle}; s) by:

$$TMP = \frac{SSA}{t_{cycle}}. \quad (10)$$

Animal preparation and instrumentation

Six adult mongrel dogs of either sex, weighing 23–37 kg, were premedicated by an intramuscular injection of Hypnorm (1 ml kg^{-1}; 1 ml Hypnorm contains 10 mg fluanisone and 0·2 mg fentanyl base). Anaesthesia was induced by an intravenous injection of pentobarbitone sodium (10 mg kg^{-1}) and maintained after endotracheal intubation with nitrous oxide (33 % O_2, 67 % N_2O) and a continuous infusion of pentobarbitone sodium (2 mg kg^{-1} h^{-1}). Ventilation was kept constant with a positive pressure respirator (Pulmomat, Dräger, Lübeck, Germany). The animal was placed on its right side, and body temperature was kept between 37·5 and 38·5 °C by means of a thermostatically regulated heating pad. A standard limb lead electrocardiogram (ECG) was used. Arterial blood samples were taken periodically to determine P_{O_2}, P_{CO_2}, pH, oxygen saturation and haemoglobin concentration using a blood gas analyser (ABL 3, Radiometer, Copenhagen, Denmark). Sodium bicarbonate solution (4·2 %) was administered intravenously to adjust the acid–base balance when necessary.

The chest was opened through the left fifth intercostal space. After removal of the fifth rib, the pericardium was opened and the heart suspended in a pericardial cradle. Epicardial bipolar platinum pacing electrodes were sutured to the heart at the right atrium, left ventricular apex, left ventricular free wall, and right ventricular outflow tract (Fig. 2).

To obtain coronary venous blood, polyethylene catheters were inserted into the distal part of the left anterior interventricular vein, draining the medial-apical part of the region of interest (Fig. 2), and into the coronary sinus.

To assess regional myocardial blood flow (see below), a Silastic catheter was placed in the left atrium for the injection of radioactively labelled microspheres. A polyethylene catheter was inserted into the right brachial artery to obtain blood for the arterial reference sample.

Left ventricular cavity and ascending aortic pressure were measured with catheter-tip micromanometers (PC-470, Millar Instruments Inc., Houston, TX, USA), inserted via the right brachial and the right femoral artery, respectively. To enable pressure calibration during the experiment, the fluid-filled lumina of the catheter-tip micromanometers were connected via three-way taps to an external pressure transducer (MS20, Electromedics Inc. Englewood, CO, USA). The third opening of the three-way tap was connected to a reference pressure level, which was the right atrial level for all pressure measurements (Arts *et al.* 1982). Ascending aortic volume flow was measured with an electromagnetic flowmeter (Skalar Transflow 601, Delft, The Netherlands).

Four inductive coils were sutured to the epicardium of the

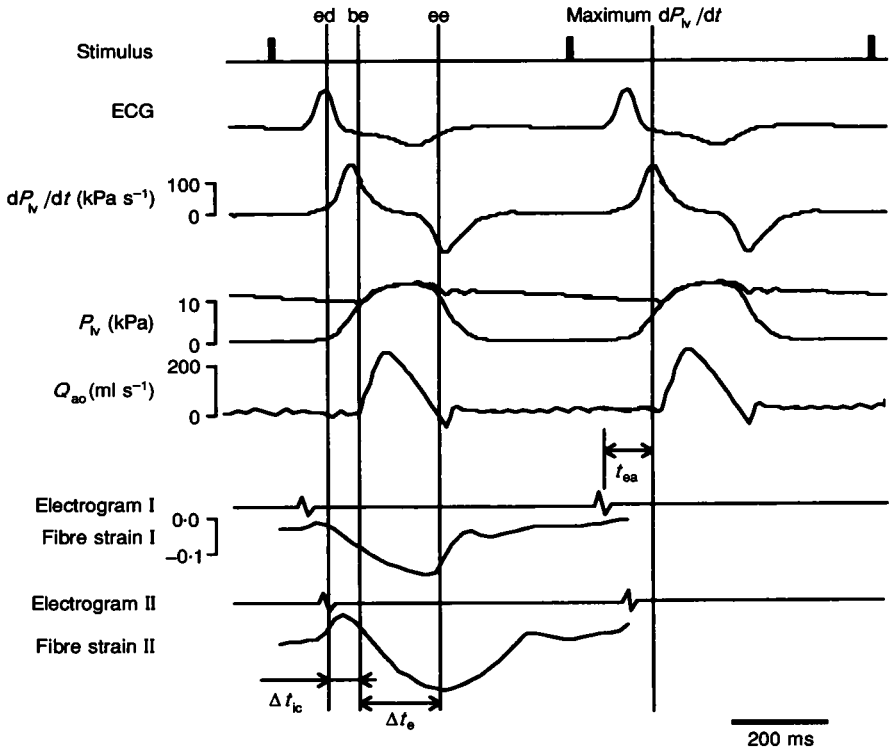

Figure 3. Typical digital recordings of haemodynamic, electrophysiological and deformation data measured during pacing at the right ventricular outflow tract

Traces from top to bottom: stimulus artifact, electrocardiogram (ECG), first derivative of left ventricular pressure (dP_{lv}/dt), left ventricular pressure (P_{lv}), instantaneous aortic volume flow (Q_{ao}), and electrogram and fibre strain in early activated basal-medial region (I) and in late activated apical-lateral region (II). In the cardiac cycle three events are determined: end-diastole (ed), begin-ejection (be) and end-ejection (ee). Δt_{ic} and Δt_e indicate the duration of the isovolumic contraction phase and the ejection phase, respectively; t_{ea} indicates the time interval between the moment of maximum dP_{lv}/dt and the moment of electrical activation.

left ventricle in a tetrahedric configuration, so that the length of each of the six edges was more or less the same. The six signals obtained from these coils were used for the determination of left ventricular cavity volume (see below).

ECG, pressure and ascending aortic volume flow signals, as well as the six signals from the inductive coils, were continuously visualized on an oscilloscope (GS-8, Knott Electronik, Hohenschäftlarn, Germany). These signals were also recorded on a paper recorder (RE 412, Schwarzer, Munich, Germany) and a multichannel tape recorder (PR2200, Ampex Corp., Redwood City, CA, USA).

Experimental protocol

For all pacing sites, minimum current levels and pace rate at which activation was regular were determined. Pacing was performed from four different sites: right atrium, left ventricular apex, left ventricular free wall and right ventricular outflow tract. During ventricular pacing the right atrium was stimulated 30 ms before the ventricle. Fifteen minutes after switching to a particular pacing site, arterial, local venous and coronary sinus blood samples were taken for blood gas analysis. Subsequently, microspheres were injected and a reference arterial sample was taken for the calculation of regional myocardial blood flow (not during left ventricular free wall pacing). Haemodynamic variables and epicardial deformation were recorded simultaneously. Within 1 min thereafter simultaneous recordings of haemodynamic variables and epicardial electrical activation were performed. The experiment was terminated by administration of an overdose of pentobarbitone sodium. Within 5 min thereafter, the heart was excised, the atria were removed from the ventricles, and the ventricles were rinsed. To determine the cavity volume of the passive left ventricle at zero transmural pressure, the left ventricle was immersed in saline, keeping the base on top, just above the saline level. Subsequently, the content of the left ventricular cavity was withdrawn with a graded syringe. Thereafter the free wall of the right ventricle was dissected, and the left ventricle was weighed.

Determination of haemodynamic variables

After performing the experiment, the haemodynamic data as recorded on analog tape were sampled (200 Hz) and digitized using a sixteen-channel twelve-bit A/D card (DASH 16G2), connected to a MS-DOS personal computer (Tulip AT Compact). Sampling and analysis were performed using a software package (ASYST 3.0, MacMillan Software Company, Rochester, NY, USA) and software developed in our laboratory. In the cardiac cycle three events were determined (Fig. 3). The end of the diastolic phase was defined as the moment before ejection at which the rate of change of left ventricular pressure (dP_{lv}/dt) exceeded 10 kPa s^{-1} (LeWinter, Kent, Kroener, Carew & Covell, 1975). The beginning of the ejection phase was determined by the moment at which left ventricular pressure exceeded end-diastolic aortic pressure. The duration of the ejection phase was determined from the aortic volume flow signal. From left ventricular pressure as a function of time, end-diastolic left ventricular pressure, maximum left ventricular pressure, and maximum first derivative of left ventricular pressure were determined. Besides these, the following haemodynamic variables were determined: heart rate, left ventricular cavity volume as a function of time (see below), maximum instantaneous ascending aortic volume flow, and ejected volume (time integral of ascending aortic volume flow).

Left ventricular cavity volume during systole was estimated as described in detail before (Delhaas *et al.* 1993*a*). In brief, the weight of the left ventricle and a two-dimensional echocardiographic image of the minor axis projection at the equator of the left ventricle were used to calculate left ventricular cavity volume at end-diastole in the control situation (right atrial pacing). Changes in end-diastolic volume as compared with this reference situation were determined using the six signals of the four inductive coils. The time course of left ventricular cavity volume during ejection was obtained by subtracting the instantaneous integral of ascending aortic volume flow from end-diastolic volume.

Precise synchronization of haemodynamic data with deformation or electrical data was performed as described previously (Delhaas *et al.* 1993*b*).

Mapping of left ventricular epicardial electrical activation pattern

A 192-electrode brush (44 × 64 mm) was used for simultaneous recording of epicardial surface electrograms at the left ventricular anterior free wall. The grid spacing between the electrodes was approximately 3·5 mm. Left ventricular pressure and ECG were recorded with the same system simultaneously with the electrode signals. Off-line, in each electrogram, the moment with the steepest negative deflection was detected and labelled by a time mark, indicating the moment of regional activation of the tissue underneath the recording electrode (Allessie, Hoeks, Schmitz & Reneman, 1986; Hoeks, Schmitz, Allessie, Jas, Hollen & Reneman, 1988). Mean regional electrical activation time was calculated for the regions as used for the deformation assessment (see below) by determining the time interval between the moment of maximum dP_{lv}/dt and the average moment of electrical activation within one region (Delhaas *et al.* 1993*b*).

During the experiment reproducible positioning of the electrode brush was obtained by visual matching of landmarks on the electrode brush with anatomical landmarks and/or video markers on the epicardial surface. Spatial matching of electrophysiological and deformation maps was enabled by four white markers, attached to the upper surface of the multi-electrode brush.

Mapping of left ventricular epicardial deformation

Two-dimensional epicardial deformation was determined with a video technique, as previously described in detail (Prinzen *et al.* 1986*b*). In brief, approximately forty white markers were attached with tissue glue (Histoacryl) to the epicardial surface of the left ventricular anterior wall. The intermarker spacing was approximately 6 mm. The area covered with markers extended 3–4 cm in the circumferential and 4–5 cm in the base-to-apex direction (Fig. 2). A video camera (Sony AVC 32500CE) with a 200 mm tele-objective, positioned at a distance of 2·5 m, and a mirror, mounted above the heart at an angle of 45 deg, were used to record the motion of the markers on a video recorder (Sony SL-C9ES, Betamax) at a speed of fifty frames per second. A video-triggered xenon flashlight illumination (Chadwick-Helmuth, Mönchengladbach, Germany) was employed to prevent motion artifacts due to smearing of the images. The direction of the epicardial fibres, being parallel to the branches of the left anterior interventricular coronary artery, and the long axis of the left ventricle, as determined by visual inspection, was indicated by a directed ruler and recorded on video during the control situation (Fig. 2). To enable synchronization of haemodynamic data with

deformation data, a frequency-modulated left ventricular pressure signal was recorded on an audio channel of the video recorder.

After the experiment sixty-four consecutive video frames (50 Hz) were digitized and stored in a 2 Mbyte digital video memory, which was coupled to a computer (PDP 11/73). Markers were detected, filtered using a singular value decomposition filtering technique (Muijtjens, Roos, Prinzen & Arts, 1990), and used for the estimation of epicardial deformation in 4×4 mutually overlapping regions by means of a least-squares criterion (Prinzen *et al.* 1986*b*). Mid-ejection of the control situation (right atrial pacing) was used as the reference state for all deformation measurements within an experiment. Natural strain in the direction of the subepicardial fibres (e_f) was calculated from epicardial deformation by:

$$e_f = \ln \frac{L_f}{L_{f,ref}}, \quad (11)$$

in which L_f and $L_{f,ref}$ represent fibre length along the subepicardial fibre direction in the actual and the reference situation, respectively. To compare myocardial fibre length in different experiments quantitatively, sarcomere length was estimated as described above.

Determination of regional myocardial blood flow

Regional myocardial blood flow was determined with radioactively labelled microspheres ($15{\cdot}0 \pm 1{\cdot}0$ μm; NEN-TRAC, DuPont DeNemours, 's-Hertogenbosch, The Netherlands), suspended in 10 % dextran with 0·01 % Tween 80 (Prinzen, Arts, van der Vusse, Coumans & Reneman, 1986*a*). The labels used were: ^{141}Ce, ^{113}Sn, ^{103}Ru, or ^{95}Nb. At each determination, 3×10^6 microspheres were injected into the left atrium. An arterial reference sample was taken from the brachial artery at a rate of 20·7 ml min^{-1}, using a Harvard withdrawal pump. Withdrawal of blood started 5 s before the injection of the microspheres, and was continued for at least 1 min.

After the experiment, the heart was fixated in 5 % formaldehyde. Before dissection, non-muscular structures, like fat and vessels at the epicardium, and chordae tendinae, were removed. The part of the left ventricular free wall with the optical markers was removed from the heart and dissected into twenty-four to thirty-six square transmural sections of approximately 7×7 mm. Each section was subdivided into a subepicardial and a subendocardial half, each of which was weighed. For the relation between regional mechanics, electrical activation and myocardial blood flow, only the subepicardial part was used. The radioactivity of the tissue and arterial blood samples was determined in a γ-counter (multichannel analyzer, Packard Europe, Brussels, Belgium). Regional subepicardial myocardial blood flow in millilitres per second per gram was calculated for the same sixteen regions as used for the determination of regional subepicardial fibre strain. Regional myocardial oxygen uptake was estimated using regional myocardial blood flow values and differences in oxygen content between blood withdrawn from the right brachial artery and the coronary sinus.

Relation between regional mechanical load and oxygen uptake

For each experiment the relation between regional oxygen uptake per second and the regional pressure–sarcomere length area or total mechanical power was expressed by a linear regression.

Statistical analysis

The effects of ventricular pacing on the variables related to haemodynamics, mechanics, myocardial blood flow and oxygen uptake were evaluated for statistical significance by applying Wilcoxon's matched-pairs signed-rank test. Values obtained during right atrial pacing in the same animal were used as reference. A difference with $P < 0{\cdot}05$ was considered to be significant (two-tailed probability). Data are presented as means ± S.D., unless indicated otherwise.

RESULTS

Influence of pacing site on haemodynamic performance

Compared with right atrial (RA) pacing, pacing at the left ventricular apex (LVA), the left ventricular free wall (LVFW) and the right ventricular outflow tract (RVOT) resulted in a significant deterioration of haemodynamic performance. Maximum left ventricular pressure decreased from $13{\cdot}2 \pm 2{\cdot}0$ to $11{\cdot}2 \pm 1{\cdot}6$, $11{\cdot}6 \pm 1{\cdot}5$ and $10{\cdot}7 \pm 2{\cdot}2$ kPa during LVA, LVFW and RVOT pacing, respectively. Maximum dP_{lv}/dt decreased from 188 ± 32 (RA) to 144 ± 15 (LVFW), 161 ± 35 (LVA) and 128 ± 26 kPa s^{-1} (RVOT). Maximum instantaneous aortic volume flow decreased from 209 ± 55 (RA) to 173 ± 37 (LVFW), 176 ± 40 (LVA) and 180 ± 60 ml s^{-1} (RVOT). Stroke volume decreased from $22{\cdot}8 \pm 4{\cdot}5$ (RA) to $18{\cdot}9 \pm 3{\cdot}2$ (LVFW), $19{\cdot}8 \pm 3{\cdot}4$ (LVA) and $19{\cdot}3 \pm 5{\cdot}4$ ml (RVOT). Heart rate, the duration of the isovolumic contraction phase and the ejection phase, and the end-diastolic left ventricular pressure were not significantly different between the various pacing modes.

Influence of pacing site on electrical activation

During right atrial pacing, electrical activation time as referred to the moment of maximum dP_{lv}/dt, was -50 ± 3 ms at the anterior left ventricular free wall. Mean values of regional electrical activation ranged between -80 and -40 ms during pacing from the three ventricular sites. Since the moment of maximum dP_{lv}/dt is used as time reference, electrical activation time is less negative in late than in early activated regions. The direction of the depolarization wave in the region of interest was highly dependent on the site of pacing. Stimulation at the right ventricular outflow tract caused a basal-medial to apical-lateral directed wave. When the heart was stimulated at the left ventricular apex, the depolarization wave was oppositely directed. During stimulation at the left ventricular free wall the depolarization wave travelled more or less perpendicular to the two former directions.

Subepicardial fibre strain and regional work during asynchronous electrical activation

In Fig. 4*A*, maps are shown of regional subepicardial fibre strain as a function of time as obtained during right atrial pacing in experiment 3. For all regions, the pattern of fibre strain was quite similar. In Fig. 4*B*, calculated regional

fibre stress is depicted as a function of time for the systolic phase of the same beat. Fibre stress increased during the isovolumic phase, reached a maximum level 40 ms after the beginning of the ejection phase and declined steadily during the rest of the ejection phase. In Fig. 4*C*, regional fibre stress is plotted as a function of fibre strain, using the data of Fig. 4*A* and *B*. The course of the loops is anticlockwise, indicating generation of mechanical work. Although during the isovolumic contraction phase global pump work was zero, regional external work during this phase appeared to be significantly different from zero, as indicated by the area under that part of the curve.

The set-up of Fig. 5 is similar to Fig. 4, but data were obtained during right ventricular outflow tract pacing in the same experiment. The pattern of fibre strain was highly dependent on the moment of electrical activation. In the

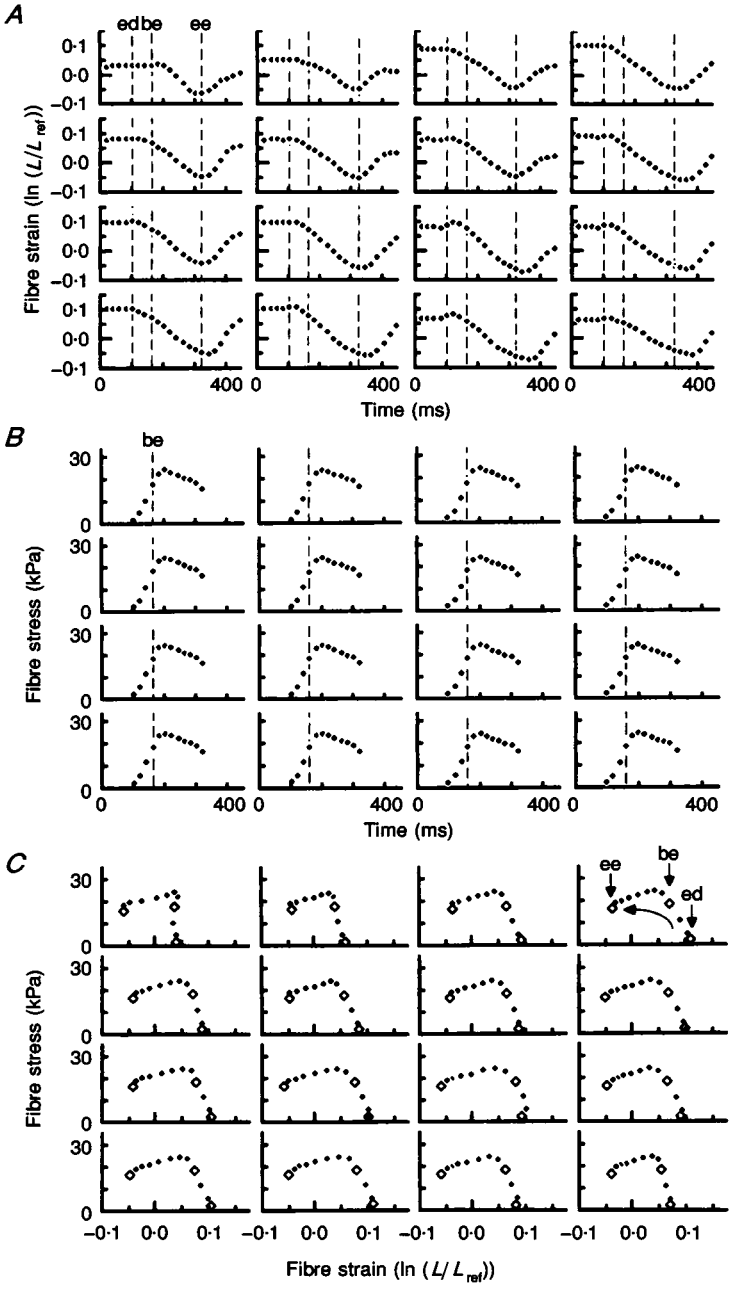

Figure 4. Regional mechanics during right atrial pacing
Maps of measured subepicardial fibre strain ($\ln(L/L_{ref})$) as a function of time (*A*), of calculated regional fibre stress as a function of time (*B*), and of calculated regional fibre stress as a function of measured fibre strain (*C*) as determined in 16 regions of the left ventricular anterior free wall in experiment 3 during right atrial pacing. The top row of signals refers to regions near the base. The left column refers to regions near the left anterior interventricular coronary artery. ed, be and ee refer to end-diastole, begin-ejection and end-ejection, respectively. The course of the loops in *C* is anticlockwise, as indicated by the arrow in the right upper plot.

early activated regions (upper region) fibres shorten markedly during the isovolumic contraction phase. During the ejection phase fibre strain in those regions was smaller than in the late activated regions. As compared with right atrial pacing, maximum fibre stress was markedly diminished and approximately the same in all regions. In Fig. 5*C*, early activated regions, as shown in the upper region, generated less external mechanical work than late activated regions.

Influence of pacing site on fibre strain, regional mechanical performance, myocardial blood flow and oxygen uptake; comparison of six experiments

The patterns of fibre strain, fibre stress, and the fibre stress–fibre strain loops, as shown in the experiment presented in Figs 4 and 5, were found in all six experiments. Maps of mean regional fibre strain during the ejection phase, estimated sarcomere length at the beginning

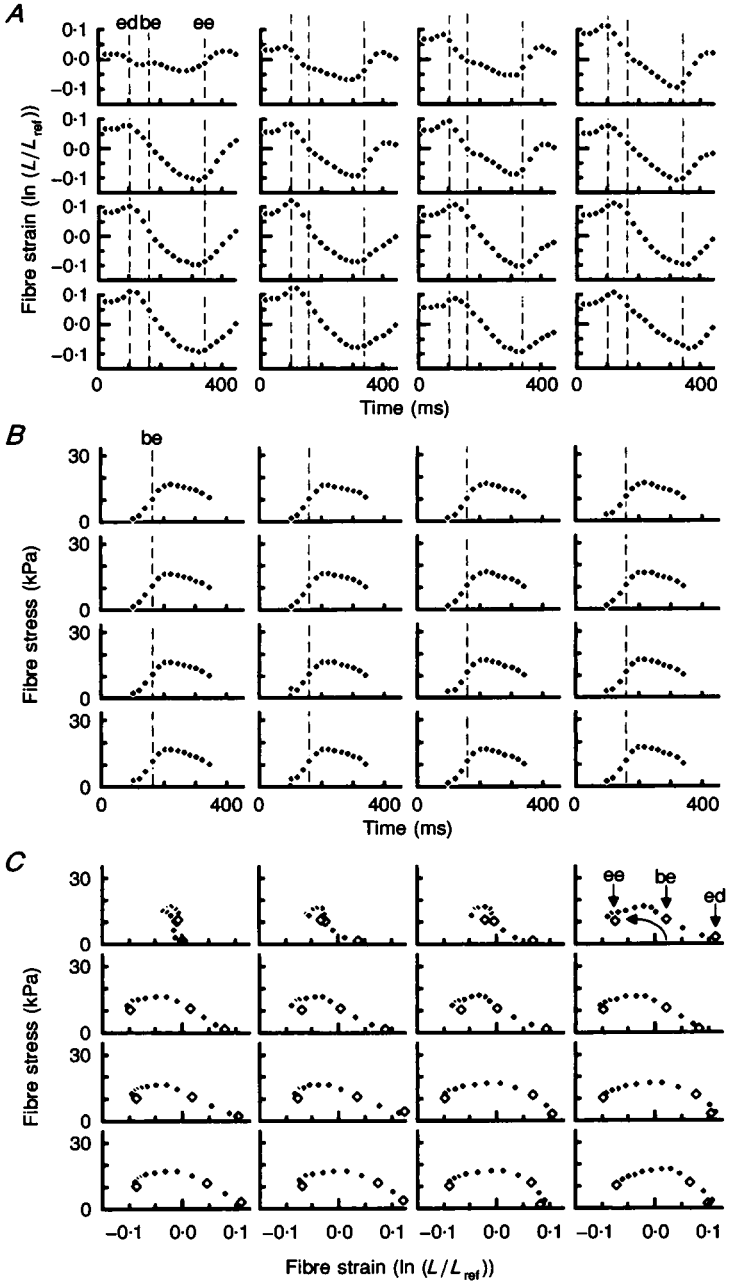

Figure 5. Regional mechanics during right ventricular outflow tract pacing
The set-up is similar to Fig. 4, but data are now obtained during right ventricular outflow tract pacing in the same experiment. *A*, fibres shorten markedly during the isovolumic contraction phase in early activated regions (upper part). During the ejection phase fibre strain in those regions was smaller than in late activated regions. *B*, compared with right atrial pacing, maximum fibre stress was markedly diminished and approximately the same in all regions. *C*, early activated regions (upper part) generate less external mechanical work than late activated regions.

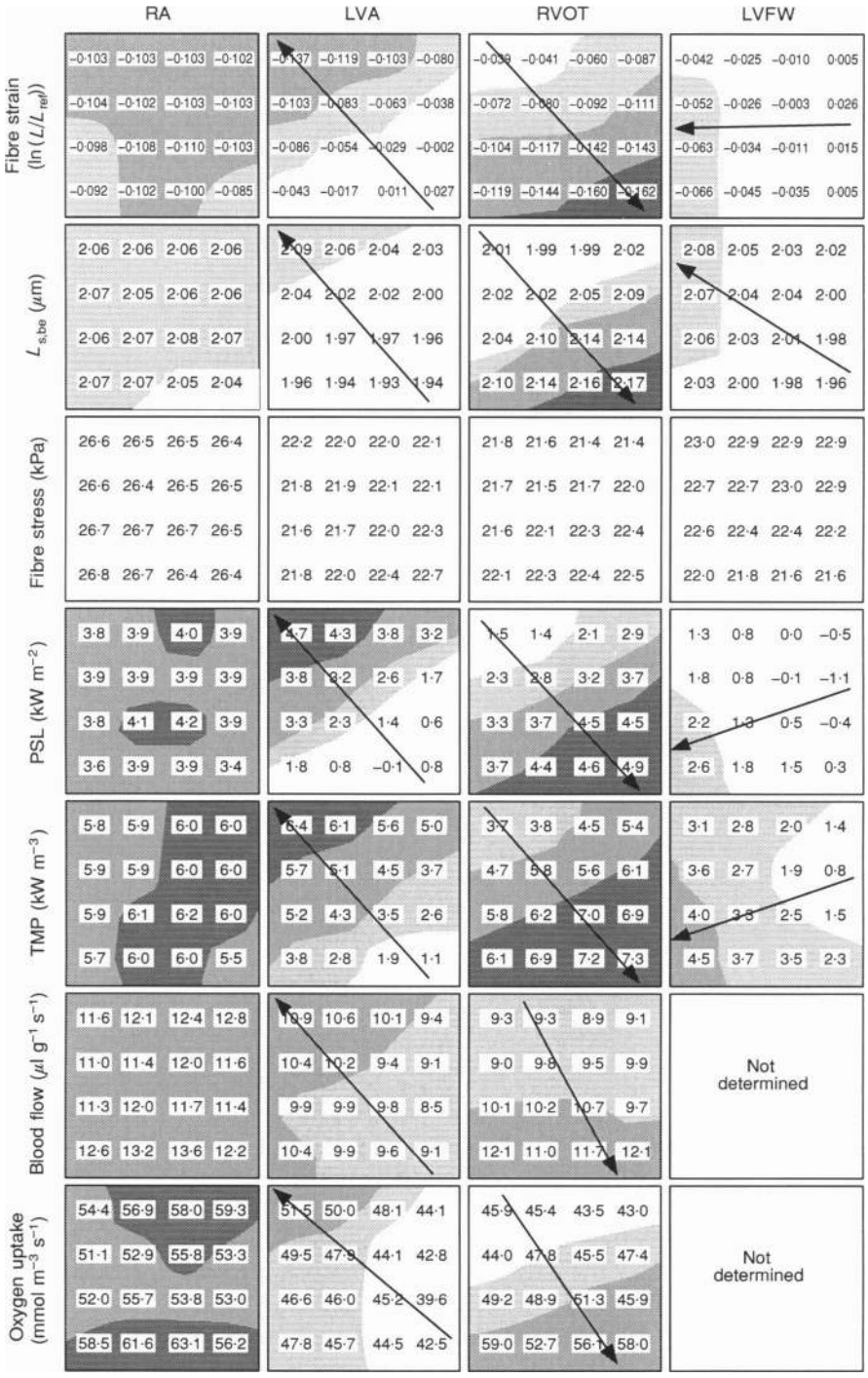

Figure 6. Mean (sub)epicardial maps of regional mechanics, blood flow and oxygen uptake
Mean (sub)epicardial maps as averaged over the 6 experiments when stimulating at the right atrium (RA), left ventricular apex (LVA), right ventricular outflow tract (RVOT), or left ventricular free wall (LVFW). Depicted are: fibre strain during the ejection phase; sarcomere length at the beginning of the ejection phase ($L_{s,be}$) estimated using eqn (6) and fibre strain measurement; fibre stress calculated using eqn (5); pressure–sarcomere length area (PSL); total mechanical power (TMP) per unit of tissue volume; regional blood flow; and regional oxygen uptake. Gradients are indicated by arrows. The boundaries between different degrees of shading indicate intervals of 0·05 in fibre strain, 0·05 μm in sarcomere length, 1·0 kW m^{-2} in PSL, 2·0 kW m^{-3} in TMP, 5 ml g^{-1} s^{-1} in blood flow, and 5 mmol m^{-3} s^{-1} in oxygen uptake.

Table 1. Values of several chemical variables in arterial (A), local venous (LV) and coronary sinus (CS) samples

	Pacing site			
Variable	RA	LVFW	LVA	RVOT
pH				
A	7·39 ± 0·04	7·37 ± 0·04	7·41 ± 0·03	7·42 ± 0·06
LV	7·36 ± 0·05	7·34 ± 0·04	7·35 ± 0·03	7·39 ± 0·05
CS	7·35 ± 0·05	7·34 ± 0·04	7·34 ± 0·04	7·38 ± 0·04
P_{CO_2} (kPa)				
A	5·0 ± 0·7	4·9 ± 0·4	5·2 ± 0·8	4·7 ± 0·7
LV	5·4 ± 1·5	6·1 ± 0·5	6·2 ± 0·7	5·7 ± 0·9
CS	6·3 ± 0·7	6·1 ± 0·6	6·2 ± 0·6	6·0 ± 0·8
Hb (mmol l^{-1})				
A	7·3 ± 1·1	6·9 ± 1·1	6·9 ± 1·3	7·1 ± 1·2
S_{O_2} (%)				
A	99 ± 0	99 ± 0	99 ± 0	99 ± 0
LV	34 ± 7	29 ± 3	32 ± 3	32 ± 6
CS	37 ± 7	31 ± 2	31 ± 3	31 ± 6
O_2 content (mmol l^{-1})				
A	7·48 ± 1·06	7·10 ± 1·10	7·09 ± 1·30	7·27 ± 1·21
LV	2·40 ± 0·72	2·09 ± 0·54	2·29 ± 0·57	2·45 ± 0·83
CS	2·80 ± 0·65	2·19 ± 0·44	2·27 ± 0·63	2·34 ± 0·76
ΔO_2 content (mmol l^{-1})				
A–LV	5·08 ± 0·60	5·02 ± 0·60	4·80 ± 0·73	4·81 ± 0·54
A–CS	4·86 ± 0·88	4·91 ± 0·76	4·83 ± 0·76	4·93 ± 0·74
O_2 extraction (%)				
LV	68 ± 7	71 ± 4	68 ± 3	67 ± 7
CS	63 ± 8	69 ± 3	69 ± 4	68 ± 7

Values are means ± S.D. Abbreviations: RA, right atrium; LVFW, left ventricular free wall; LVA, left ventricular apex; RVOT, right ventricular outflow tract; Hb, haemoglobin; S_{O_2}, oxygen saturation.

of the ejection phase, maximum active fibre stress, pressure–sarcomere length area, total mechanical power, subepicardial blood flow, and oxygen uptake are shown in Fig. 6 for right atrial, left ventricular apex, right ventricular outflow tract and left ventricular free wall pacing. As indicated by the shading pattern, during right atrial pacing some regional differences were present in the variables presented. However, using two-dimensional analysis, in none of the variables presented could a gradient be found. During pacing from ventricular sites, however, mean values of mechanical variables and oxygen uptake were markedly decreased in the early activated regions, except for estimated maximum fibre stress. The gradients, depicted in Fig. 6, pointed towards the same direction as the depolarization wave. On average, fibre lengthening during the ejection phase was observed in the early activated areas while the hearts were paced at the left ventricular free wall or the left ventricular apex. Therefore, regional external work was negative in these regions. In each experiment the non-uniformities due to the asynchronous electrical activation were generally larger than as indicated by the mean values for each region, because the position of the region with the lowest and highest values varied for each experiment.

In Table 1, values of pH, P_{CO_2}, Hb, oxygen saturation, oxygen content, arteriovenous difference in oxygen content, and of oxygen extraction are shown for the different pacing modes using arterial, local venous and coronary sinus blood samples. None of the variables presented was significantly affected by ventricular pacing. Moreover, no significant differences could be detected between these biochemical variables as measured in local venous blood and in coronary sinus blood.

Relation between regional mechanical indices and oxygen uptake

Ninety-five per cent confidence intervals of the relation between regional oxygen uptake and the regional pressure–sarcomere length area or total mechanical power obtained during pacing at the right atrium, the left ventricular apex and the right ventricular outflow tract in six experiments are plotted in Fig. 7*A* and *B*, respectively. As a result of the variation in haemodynamic conditions in the different experiments, data were obtained during a variety of

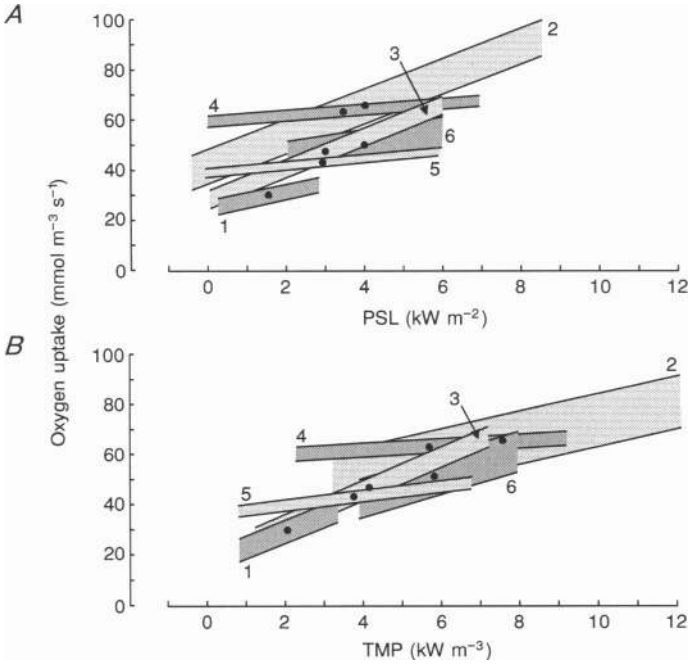

Figure 7. Ninety-five per cent confidence intervals of correlation between oxygen uptake and pressure–sarcomere length area or total mechanical power
Ninety-five per cent confidence intervals of correlation between oxygen uptake and pressure–sarcomere length area (*A*) or total mechanical power (*B*), as measured in all 6 experiments during right atrial, left ventricular apex and right ventricular outflow tract pacing. Numbers refer to the experiments as mentioned in Table 2. ●, centres of the estimated relations.

loading conditions, heart rates and contractile conditions. Also, different patterns of electrical activation were investigated. The pressure–sarcomere length area ranged from −0·4 to 8·7 kW m^{-2}, total mechanical power from 0·5 to 12·5 kW m^{-3} and regional oxygen uptake from 10 to 120 mmol m^{-3} s^{-1}. The correlation coefficients of the relations between the pressure–sarcomere length area and regional oxygen uptake within the individual experiments did not significantly differ from the ones between total mechanical power and regional oxygen uptake. Since there were differences in offset of the centres of the relations between the pressure–sarcomere length area and regional oxygen uptake, the linear relation obtained from the pooled data holds only for the relation between total mechanical power (TMP) and regional oxygen uptake ($\dot{V}_{O_2,reg}$), revealing the following linear regression:

$$\dot{V}_{O_2,reg} = k_1 TMP + k_2, \quad (12)$$

with

$k_1 = 4{\cdot}94 \pm 0{\cdot}31$ mol J^{-1} and $k_2 = 24{\cdot}2 \pm 1{\cdot}9$ mmol m^{-3} s^{-1}.

The regression coefficient was 0·68. Table 2 shows the coefficients of the linear regression lines of the relation between measured regional oxygen uptake and total mechanical power as estimated for the individual experiments, and for the pooled data. Within the experiments correlations were less than for the pooled data. Table 2 also shows the coefficients of the linear regression lines of the relation between measured regional oxygen uptake and the pressure–sarcomere length area.

DISCUSSION

In the present study a new method is proposed and applied to estimate regional fibre stress in the left ventricular wall. The second and main goal was to find a proper index of regional oxygen demand in the subepicardial layers of the anterior free wall of the left ventricle. To obtain regional differences in mechanical performance, the hearts were paced from the right atrium and various ventricular sites. In early activated regions, both regional oxygen uptake and regional mechanical work were significantly less than in late activated regions. The pressure–sarcomere length area and total mechanical power, an index obtained from the time curve of estimated fibre stress and fibre strain in analogy to the pressure–volume area of Suga and co-workers (Suga, 1979; Suga *et al.* 1981*a*, *b*), were related to regional oxygen consumption as estimated from regional subepicardial blood flow and arterio-coronary sinus differences in oxygen content. In an individual experiment the correlation between the pressure–sarcomere length area and regional oxygen uptake was not significantly different from that between total mechanical power and regional oxygen uptake. However, pooling of the linear relations between the pressure–sarcomere length area and regional oxygen uptake does not reveal a reliable relation

Table 2. Coefficients (SE) of estimated linear relation between regional oxygen demand and total mechanical power (TMP) or pressure–sarcomere length area (PSL)

	TMP			PSL		
Experiment	Slope (mol J^{-1})	Intercept (mmol m^{-3} s^{-1})	r	Slope (mol J^{-1} m^{-1})	Intercept (mmol m^{-3} s^{-1})	r
1	6·71 (2·51)	15·78 (5·55)	0·37	3·42 (1·96)	24·83 (3·37)	0·25
2	4·69 (1·34)	25·96 (12·13)	0·46	6·00 (1·51)	41·92 (7·16)	0·50
3	7·05 (0·85)	17·47 (3·76)	0·77	6·33 (1·09)	28·37 (3·51)	0·65
4	1·38 (0·65)	55·54 (4·14)	0·30	1·22 (0·54)	59·77 (2·19)	0·31
5	2·43 (0·66)	33·68 (2·80)	0·48	1·56 (0·50)	38·94 (1·70)	0·42
6	5·65 (1·41)	13·61 (9·26)	0·51	2·48 (1·52)	40·58 (6·24)	0·23
Mean	4·94 (0·31)	24·24 (1·85)	0·68	5·53 (0·52)	32·78 (1·90)	0·53

Values given in parentheses are standard errors of the estimate.

because of the differences in offset of the centre of the individual relations. The results suggest that regional total mechanical power is a better and more general estimate of regional oxygen demand than the pressure–sarcomere length area.

Calculation of regional stress has not been commonly applied. Most calculation methods use local radii of curvature, wall thickness, regional material properties and ventricular pressure. In the present study, a method has been proposed to estimate regional fibre stress during systole from calculated average fibre stress and measured regional fibre strain. In estimating regional fibre stress it was assumed that the distribution of force acting in the fibre direction, defined as Cauchy fibre stress multiplied by cross-sectional area of the myocardial fibre bundle, is homogeneously distributed because of a free conductance of force along the fibre bundle. This assumption is especially important in the case of ventricular pacing. Then electrical activation is asynchronous, causing fibre strain to become non-uniform. Despite spatial differences in fibre strain during ventricular pacing (Fig. 6), no significant spatial gradient could be calculated for regional maximum fibre stress. This can be explained as follows. The inhomogeneous fibre shortening during asynchronous electrical activation caused differences in sarcomere length at the moment that average fibre stress according to eqn (1) was maximal. These differences in sarcomere length did not have a gradient in spatial distribution. Estimated sarcomere length at this moment ranged from 1·82 to 2·20 μm (median 2·01 μm), while regional differences in length within a cardiac cycle analysed ranged from 0·05 to 0·20 μm (median 0·08 μm). According to eqn (5) differences in maximum Cauchy fibre stress ranged from 2 to 10 % (median 5 %).

The stress in the myocardial fibres is calculated as the sum of axial and circumferential stress minus twice the radial stress (Arts *et al.* 1982, 1991). If the fibres are embedded in soft incompressible material, this stress is exactly the same as the stress in the fibres. If the embedding material is stiffer, thus simulating shear force interaction between the fibres, the stress as calculated is still an accurate predictor of the stress related to generation of regional mechanical work by the tissue (Arts *et al.* 1982, 1991), which is just the parameter we are interested in. When using the equations for segmental calculation of left ventricular wall stress as presented by Regen and co-workers (Regen, Anversa & Capasso, 1993), fibre stress was found to be twice as low. However, in this approach fibre stress is defined as the average of meridional and hoop stress, whereas in our method it is defined as the stress in the fibres, which is the sum of axial and circumferential minus twice the radial stress. Because radial stress is almost zero in the subepicardial layers, Regen's values and ours are essentially the same.

Since direct experimental measurement of fibre stress is practically impossible, mathematical models of the mechanics of the left ventricle are often used to estimate fibre stress. When using experimentally determined mechanical properties of myocardial material, in such a model, the distribution of fibre stress appeared to be quite uniform, even if activation of the left ventricle was asynchronous (Bovendeerd, 1990). The distribution of fibre strain during the ejection phase, however, was found to vary significantly with changes in activation time.

Regional contractile work has been estimated by calculating the area within the loop described by plotting left ventricular pressure as a function of regionally measured sarcomere or segment length (Theroux *et al.* 1974; Tyberg *et al.* 1974; Badke *et al.* 1980; Lew, 1987). Although the presence of a loop indicates generation of mechanical work, the quantitative value is limited. After all, left ventricular pressure is not a proper representative of myocardial fibre stress because of unknown and variable geometric factors. Furthermore, measured segment length is proportional to the more or less arbitrary length in the reference state. As a result, within one experiment the method may be used to obtain an indication of changes in

Table 3. Experimentally derived values of left ventricular cavity volume at zero transmural pressure (V_{eq}), of wall volume (V_w) and of extrapolated sarcomere length at zero left ventricular cavity volume ($L_{s,0}$), using eqn (2)

Experiment	V_{eq} (ml)	V_w (ml)	V_{eq}/V_w	$L_{s,0}$ (μm)
1	42	109·5	0·38	1·51
2	38	135·2	0·28	1·59
3	34	122·9	0·28	1·59
4	47	158·1	0·30	1·58
5	34	147·6	0·23	1·64
6	31	118·1	0·26	1·61
Mean ± S.D.	—	—	0·29 ± 0·05	1·59 ± 0·04

regional work during the experiment, but comparison between different hearts is impossible. Hence, in two animals with equal stroke volume and time course of left ventricular pressure, but with different left ventricular wall and cavity volume, the same oxygen consumption will be calculated using the pressure–length area, although the animal with the lowest left ventricular cavity to wall volume ratio is expected to have a lower fibre stress, and, consequently, a lower oxygen consumption.

In calculating the pressure–volume area, the left ventricular cavity volume below which no active pressure can be developed ($V_{lv,d}$) may be set to zero without introducing large errors (Suga *et al.* 1981*a*, *b*). Using the values of measured left ventricular cavity volume at passive zero transmural pressure in eqn (2), estimated sarcomere length at zero left ventricular cavity volume was found to be 1·59 ± 0·04 μm (Table 3). This is not significantly different from 1·60 μm, which is the sarcomere length at which active fibre stress is assumed to be zero (Pollack & Krueger, 1976).

The areas of the fibre stress–fibre strain loops in Fig. 5*C* consistently show an increase in size from early to late activated regions. So, late activated areas are likely to have a higher oxygen demand, which is supported by the finding that the distributions of regional total mechanical power, blood flow and oxygen uptake show a similar pattern. The present data indicate that the low myocardial blood flow and oxygen uptake values in early activated regions are determined by the lower demands in these regions. First of all, fibre stress is not higher in early than in late activated regions (Fig. 6). Therefore, a larger compression of the microcirculation in early activated regions is not likely to be the cause of the lower blood flow. Moreover, the present study deals with blood flow in the subepicardial layers of the left ventricular free wall, which is known to be hardly affected by cardiac contraction. If early activation had induced underperfusion, one would expect increased oxygen extraction and increased P_{CO_2} in the locally sampled venous blood in the case of left ventricular apex pacing. However, this was not the case (Table 1). This finding is in accordance with the finding that altered myocardial oxygen demand generally induces a change in coronary blood flow rather than in oxygen extraction (Braunwald, 1971; Feigl, 1983). However, despite simultaneous withdrawal of blood from the local vein and the coronary sinus, it cannot be excluded that through the local venous catheter, blood is also sampled from adjacent vascular beds via venous collaterals. If mixing with blood from adjacent areas occurs, changes due to asynchronous electrical activation will be underestimated. More detailed lateral and transmural mapping of oxygen uptake, for example using the microspectrometry technique developed by Weiss and co-workers (Weiss, Neubauer, Lipp & Sinha, 1978), is ultimately required to investigate the influence of asynchronous electrical activation on oxygen uptake.

The lower mechanical power in the early activated regions may be explained as follows. In early activated regions, the initial contraction is almost isotonic. The resulting smaller sarcomere length at the beginning of the ejection phase may be responsible for the absence of increased fibre stress during the ejection phase, although the sarcomeres contract isometrically (Figs 5 and 6). Due to isometric contraction during ejection in early activated regions, external power is lower in early than in late activated regions. Since maximum fibre stress and sarcomere length at the end of the ejection phase are approximately the same in early and in late activated regions (Fig. 6), potential power is also approximately the same for all regions. Therefore, total mechanical power, being the sum of external and potential power, is lower in early than in late activated regions (Fig. 6).

Despite a fairly good overall relation between total mechanical power and regional oxygen uptake ($r = 0·68$), as shown in Table 2 and Fig. 7*B*, within the experiments the correlation was not always so high. One of the most important causes for this phenomenon is that the range in regional total mechanical power and oxygen uptake within an experiment was rather small. An alternative explanation for the varying reliability of the relation between oxygen uptake and total mechanical power is the difference in site of determination of oxygen uptake and deformation. Oxygen uptake was calculated from myocardial blood flow, as regionally measured in the subepicardial half of the left ventricular wall, and the

Table 4. Comparison of total mechanical power (TMP)–regional oxygen demand relation with pressure–volume area (PVA)–global oxygen demand relation as presented in literature

Study	Procedure	(Non-) ejecting	Species	Slope (mol J^{-1})	Intercept (mmol m^{-3} s^{-1})
Present study	SSA	Ejecting	Dog	4·65	25·7
Suga (1979)	PVA	Ejecting	Dog	4·16	18·3
Suga *et al.* (1983)	PVA	Ejecting	Dog	4·62	22·9
Khalafbeigui *et al.* (1979)	PVA	Non-ejecting	Dog	4·64	13·0
Goto *et al.* (1988)	PVA	Non-ejecting	Rabbit	5·76	26·9

arterio-coronary sinus difference in oxygen content. The regional fibre stress–fibre strain area was determined at the epicardial surface. Since no differences were found between the biochemical variables measured in the blood samples from the local coronary vein and the coronary sinus (Table 1), the blood sample from the coronary sinus was regarded as being representative of the whole heart, even during asynchronous electrical activation. Since oxygen consumption was estimated from regionally measured blood flow and arterio-coronary sinus differences in oxygen content, regional oxygen uptake is mainly a function of the microsphere distribution. However, from experiment to experiment and, within each experiment, from pacing mode to pacing mode, random differences in arterio-venous differences in oxygen content were detected. Therefore, both components of oxygen uptake, blood flow and oxygen extraction, are taken into account as far as the relation with the regional indices of contractile work is concerned.

The relation between regional total mechanical power and regional myocardial oxygen uptake, obtained by pooling all data, is in quantitative agreement with the relations as described between the pressure–volume area and global cardiac oxygen demand (Table 4) (Khalafbeigui *et al.* 1979; Suga, 1979; Suga *et al.* 1983; Goto, Slinker & LeWinter, 1988). In those studies, energy units of the pressure–volume area and oxygen uptake were millimetres of mercury × millilitres and millilitres of O_2, respectively. These units were converted into the units as used in this study, assuming that the values of oxygen uptake were given in millilitres at 273 K and at 1 atm. The similarity of the relations provides evidence that regional total mechanical power can be used to estimate regional oxygen demand.

Conclusions

Regional fibre stress in the subepicardial half of the left ventricular wall during synchronous as well as asynchronous electrical activation can be calculated from left ventricular pressure, left ventricular cavity and wall volume, and regional subepicardial fibre strain. Regional fibre stress thus calculated during asynchronous electrical activation is quite uniformly distributed, despite large differences in regional fibre strain. During asynchronous electrical activation, regional contractile work, myocardial blood flow and oxygen uptake were significantly lower in early than in late activated regions. Using values of regionally measured fibre strain and calculated fibre stress, regional oxygen demand can be estimated from the fibre stress–fibre strain area in analogy to the estimation of global left ventricular oxygen demand on the basis of left ventricular pressure and volume according to Suga and co-workers (Suga, 1979; Suga *et al.* 1981*a*, *b*). Division of the fibre stress–fibre strain area by the duration of the cardiac cycle reveals regional total mechanical power (TMP). When determining regional oxygen uptake ($\dot{V}_{O_2,reg}$) as the product of regional myocardial blood flow and arterio-coronary sinus difference in oxygen content, it is found that $\dot{V}_{O_2,reg} = k_1\,TMP + k_2$, with $k_1 = 4{\cdot}94 \pm 0{\cdot}31$ mol J^{-1} and $k_2 = 24{\cdot}2 \pm 1{\cdot}9$ mmol m^{-3} s^{-1}. This relation between regional total mechanical power and myocardial oxygen demand is in quantitative agreement with previously reported relations between global oxygen demand and measured pressure–volume area. The results indicate that asynchronous electrical activation causes a redistribution of mechanical work and oxygen demand and that regional total mechanical power is a better and more general estimate of regional oxygen demand than the pressure–sarcomere length area.

REFERENCES

Allessie, M. A., Hoeks, A. P. G., Schmitz, G. M. L. & Reneman, R. S. (1986). On-line mapping system for the visualization of the electrical activation of the heart. *International Journal of Cardiac Imaging* **2**, 59–63.

Arts, T., Bovendeerd, P. H. M., Prinzen, F. W. & Reneman, R. S. (1991). Relation between left ventricular cavity pressure and volume and systolic fiber stress and strain in the wall. *Biophysical Journal* **59**, 93–102.

Arts, T. & Reneman, R. S. (1980). Measurement of deformation of canine epicardium *in vivo* during cardiac cycle. *American Journal of Physiology* **239**, H432–437.

Arts, T., Veenstra, P. C. & Reneman, R. S. (1982). Epicardial deformation and left ventricular wall mechanics during ejection in the dog. *American Journal of Physiology* **243**, H379–390.

Badke, F. R., Boinay, P. & Covell, J. W. (1980). Effect of ventricular pacing on regional left ventricular performance in the dog. *American Journal of Physiology* **238**, H858–867.

Bovendeerd, P. H. M. (1990). The mechanics of the normal and ischemic left ventricle during the cardiac cycle. PhD Thesis, University of Limburg, Maastricht, The Netherlands.

BRAUNWALD, E. (1971). Control of myocardial oxygen consumption. *American Journal of Cardiology* **27**, 416–432.

CHADWICK, R. S. (1982). Mechanics of the left ventricle. *Biophysical Journal* **39**, 279–288.

DELHAAS, T., ARTS, T., BOVENDEERD, P. H. M., PRINZEN, F. W. & RENEMAN, R. S. (1993*a*). Subepicardial fiber stress and strain as related to left ventricular pressure and volume. *American Journal of Physiology* **264**, H1548–1559.

DELHAAS, T., ARTS, T., PRINZEN, F. W. & RENEMAN, R. S. (1993*b*). Relation between regional electrical activation time and subepicardial fiber strain in the canine left ventricle. *Pflügers Archiv* **423**, 78–87.

FEIGL, E. O. (1983). Coronary physiology. *Physiological Reviews* **63**, 1–205.

FEIGL, E. O., SIMON, G. A. & FRY, D. L. (1967). Auxotonic and isometric cardiac force transducers. *Journal of Applied Physiology* **23**, 597–600.

GALLAGHER, K. P., OSAKADA, G., MATSUZAKI, M., KEMPER, W. S. & ROSS, J. JR (1982). Myocardial blood flow and function with critical coronary stenosis in exercising dogs. *American Journal of Physiology* **243**, H698–707.

GOTO, Y., SLINKER, B. K. & LEWINTER, M. M. (1988). Similar normalized E_{max} and O_2 consumption–pressure–volume area relation in rabbit and dog. *American Journal of Physiology* **255**, H366–374.

GRIMM, A. F., LIN, H. L. & GRIMM, B. R. (1980). Left ventricular free wall and intraventricular pressure sarcomere length distributions. *American Journal of Physiology* **239**, H101–107.

HATA, K., GOTO, Y. & SUGA, H. (1991). External mechanical work during relaxation period does not affect myocardial oxygen consumption. *American Journal of Physiology* **261**, H1778–1784.

HISANO, R. & COOPER, G. (1987). Correlation of force–length area with oxygen consumption in ferret papillary muscle. *Circulation Research* **61**, 318–328.

HOEKS, A. P. G., SCHMITZ, G. M. L., ALLESSIE, M. A., JAS, H., HOLLEN, S. J. & RENEMAN, R. S. (1988). Multichannel storage and display system to record the electrical activity of the heart. *Medical and Biological Engineering and Computing* **26**, 434–438.

HUISMAN, R. M., ELZINGA, G., WESTERHOF, N. & SIPKEMA, P. (1980). Measurement of left ventricular wall stress. *Cardiovascular Research* **14**, 142–153.

KHALAFBEIGUI, F., SUGA, H. & SAGAWA, K. (1979). Left ventricular systolic pressure–volume area correlates with oxygen consumption. *American Journal of Physiology* **237**, H566–569.

LEW, W. Y. W. (1987). Influence of ischemic zone size on nonischemic area function in the canine left ventricle. *American Journal of Physiology* **252**, H990–997.

LEWINTER, M. M., KENT, R. S., KROENER, J. M., CAREW, T. E. & COVELL, J. W. (1975). Regional differences in myocardial performance in the left ventricle of the dog. *Circulation Research* **37**, 191–199.

LISTER, J. W., KLOTZ, D. H., JOMAIN, S. L., STUCKEY, J. H. & HOFFMAN, B. (1964). Effect of pacemaker site on cardiac output and ventricular activation in dogs with complete heart block. *American Journal of Cardiology* **14**, 494–503.

MUIJTJENS, A. M. M., ROOS, J. M. A., PRINZEN, T. T. & ARTS, T. (1990). Noise reduction in estimating epicardial deformation from marker tracks. *American Journal of Physiology* **258**, H599–605.

PANERAI, R. B. (1980). A model of cardiac muscle mechanics and energetics. *Journal of Biomechanics* **13**, 929–940.

PARMLEY, W. W. & TYBERG, J. V. (1976). Determinants of myocardial oxygen demand. *Progress in Cardiology* **5**, 19–36.

POLLACK, G. H. & KRUEGER, J. W. (1976). Sarcomere dynamics in intact cardiac muscle. *European Journal of Cardiology* **4**, suppl., 53–65.

PRINZEN, F. W., ARTS, T., VAN DER VUSSE, G. J., COUMANS, W. A. & RENEMAN, R. S. (1986*a*). Gradients in fiber shortening and metabolism across ischemic left ventricular wall. *American Journal of Physiology* **250**, H255–264.

PRINZEN, T. T., ARTS, T., PRINZEN, F. W. & RENEMAN, R. S. (1986*b*). Mapping of epicardial deformation using a video processing technique. *Journal of Biomechanics* **19**, 263–273.

PRINZEN, F. W., AUGUSTIJN, C. H., ARTS, T., ALLESSIE, M. A. & RENEMAN, R. S. (1990). Redistribution of myocardial fiber strain and blood flow by asynchronous electrical activation. *American Journal of Physiology* **259**, H300–308.

REGEN, D. M., ANVERSA, P. & CAPASSO, J. M. (1993). Segmental calculation of left ventricular wall stresses. *American Journal of Physiology* **264**, H1411–1421.

SPOTNITZ, H. M., SONNENBLICK, E. H. & SPIRO, D. (1966). Relation of ultrastructure to function of the intact heart. Sarcomere structure relative to pressure–volume curves of intact left ventricles of dog and cat. *Circulation Research* **18**, 49–66.

SUGA, H. (1979). Total mechanical energy of a ventricle model and cardiac oxygen consumption. *American Journal of Physiology* **236**, H498–505.

SUGA, H., HAYASHI, T. & SHIRAHATA, M. (1981*a*). Ventricular systolic pressure–volume area as predictor of cardiac oxygen consumption. *American Journal of Physiology* **240**, H39–44.

SUGA, H., HAYASHI, T., SHIRAHATA, M., SUEHIRO, S. & HISANO, R. (1981*b*). Regression of cardiac oxygen consumption on ventricular pressure–volume area in dog. *American Journal of Physiology* **240**, H320–325.

SUGA, H., HISANO, R., HIRATA, S., HAYASHI, T., YAMADA, O. & NINOMIYA, I. (1983). Heart rate-independent energetics and systolic pressure–volume area in dog heart. *American Journal of Physiology* **244**, H206–214.

TER KEURS, H. E. D. J., RIJNSBURGER, W. H., VAN HEUNINGEN, R. & NAGELSMIT, M. J. (1980). Tension development and sarcomere length in rat cardiac trabeculae; evidence of length-dependent activation. *Circulation Research* **46**, 703–714.

THEROUX, P., FRANKLIN, D., ROSS, J. J. & KEMPER, W. S. (1974). Regional myocardial function during acute coronary artery occlusion and its modification by pharmacologic agents in the dog. *Circulation Research* **35**, 896–908.

TYBERG, J. V., FORRESTER, J. S., WYATT, H. L., GOLDNER, S. J., PARMLEY, W. W. & SWAN, H. J. C. (1974). An analysis of segmental dysfunction utilizing the pressure–length loop. *Circulation* **49**, 748–754.

VAN HEUNINGEN, R., RIJNSBURGER, W. H. & TER KEURS, H. E. D. J. (1982). Sarcomere length control in striated muscle. *American Journal of Physiology* **242**, H411–420.

WEBER, K. T. (1979). The metabolic demand and oxygen supply of the heart: physiologic and clinical considerations. *American Journal of Cardiology* **44**, 722–729.

WEISS, H. R., NEUBAUER, J. A., LIPP, J. A. & SINHA, A. K. (1978). Quantitative determination of regional oxygen consumption in the dog heart. *Circulation Research* **42**, 394–401.

WIGGERS, C. J. (1925). The muscular reactions of the mammalian ventricles to artificial surface stimuli. *American Journal of Physiology* **73**, 346–378.

Acknowledgement

This work was supported by NWO grant 900-516-091.

Received 6 May 1993; accepted 9 November 1993.